



Measurement of Releasing Radon gas at Archaeological Site in Egypt and its Associated Radiation Dose

Hassan, N. M.^{1,2*}; Salama, S.;³ and Al-Deeb, A.¹

Received: 11/04/2022

Accepted: 09/06/2022

DOI: 10.21608/jntas.2022.131348.1051

E.mail:nmmh1976@Zu.edu.eg

ABSTRACT

Radon concentration at Tanis, Sharqai, Egypt, was measured at the site as well as at the laboratory using a sealed CAN-technique equipped CR-39 detector which was calibrated in advance. In situ measured radon concentration ranged from 72 ± 9 Bq m⁻³ to 144 ± 16 Bq m⁻³, while the equilibrium radon concentration of 20 soil samples collected from the same sites were ranged from 88 ± 12 Bq m⁻³ to 226 ± 36 Bq m⁻³ at the laboratory. The average radon concentration is less than the recommended value by ICRP of 300 Bq m⁻³ but it is higher than the recommended value by WHO of 100 Bq m⁻³. The radon exhalation rate was ranged from $(24 \pm 3$ to $61 \pm 10) 10^{-4}$ Bq m² s⁻¹. It shows a good correlation with the radium content of a linear correlation factor of $R = 0.97$, which implies, the radium content is a useful index for radon parameters. Moreover, the radiation dose was calculated using radon concentration at sites and its value was ranged from 0.40 ± 0.05 to 0.79 ± 0.09 mSv y⁻¹ for workers and from 0.054 ± 0.007 to 0.108 ± 0.012 mSv y⁻¹ for visitors. From the obtained results, we assure there is no radiation health hazard from visiting the studied archaeological site.

KEYWORDS

*Radon, Radiation
Dose, CAN-technique,
Soil, Archaeological
Site.*

1. Department of Physics, Faculty of Science, Zagazig University, Zagazig, P.O. Box 44519, Egypt
2. Department of Physics, Faculty of Science, University of Bahrain, P.O. Box 32038, Kingdom of Bahrain
3. Radiation Protection & Civil Defense, Nuclear Research Center, Egyptian Atomic Energy Authority, Egypt

INTRODUCTION

A high awareness is raised among several nations about the radiation dose delivered to the population from the naturally occurring radioactive gas, radon (^{222}Rn ; $T_{1/2} \approx 3.82$ d), which is born from radium (^{226}Ra) decaying; a member of uranium (^{238}U) series (Nazaroff, 1992). Radon alone contributes to more than 50% of the total radiation dose received by individuals from natural radiation sources (worldwide average natural dose of human is $1.4\text{--}2.4$ mSv y^{-1}) (UNSCEAR, 2000). Radon concentration in the air varies as a function of radium content in soil, rocks or in building materials (Hassan et al., 2009). For instance, radon gas can be accumulated in confined spaces, particularly closed space or dwelling places and becomes a significant source of internal radiation exposure; as is the case in many tourist places, including the Egyptian Tanis. The city of Tanis is relatively unknown among Egypt's wealth of historical sites, though it yielded one of the greatest archeological troves ever found. Once the capital of all Egypt, Tanis's royal tombs have yielded artifacts on par with the treasures of Tutankhamun. Naturally, radon decays to short-lived of ^{218}Po , ^{214}Pb , ^{214}Bi and ^{214}Po , which have properties of spreading and attaching to aerosols (Nazaroff, 1992). More critically these short-lived decay products could finally trap into lung walls or bronchial tissues that cause high risk of radiogenic lung Cancer by depositing their alpha-particle energies through the lung tissues (Durrani et al., 1987; Sahu et al., 2016; Abo-Elmagd et al., 2018). (UNSCEAR, 2008; ICRP, 2010) reported a strong correlation between residential radon concentration and lung cancer. In addition, (WHO, 2005), identified radioactive radon gas as the second leading cause of lung Cancer next to tobacco smoking. Therefore, due to the impact of radiological hazard of radon, the accurate evaluation of radon concentration of materials is important. It is also essential to understand the generation and migration

mechanisms of radon and the factors that influence these pathways (Hassan, 2014).

Radon emanation coefficient is the ratio of radon amount enters the pore spaces to the total radon amount generated from radium decay in solid grains (Hassan, 2014; Hosoda et al., 2009). Generally, in a solid grain, when naturally occurred radon gas generated from radium decay a fraction of radon gas penetrates into the pore spaces between these solid grains. The emanation coefficient is highly influenced by water content. For example, increasing the water amount in the pore spaces causes upsurges in the probability of capturing radon atoms within pore spaces (Nazaroff, 1992; Hassan, 2014). Consequently, before radon atoms undergo natural radioactive decay, some of them migrate to the atmosphere; that is, the radon is exhaled from the surface of the materials. The exhalation rate is defined as the amount of releasing radon per unit surface area per unit time (Schery et al., 1989; Sasaki et al., 2004). The emanation coefficient and the exhalation rates can control the amount of radon in the atmosphere.

Various analytical techniques have been reported in the literature for measuring radon concentrations in the air that released from environmental materials. Among the reported active techniques, an accumulation chamber equipped with a scintillation cell monitor (Lucas cell Model 300 A + Radiation monitor Model AB-5, Pylon Electrics, Inc., Ottawa, Canada) (Hassan et al., 2009; Hassan, 2014; Hosoda et al., 2009), Alpha Guard (Saphymo, Germany), a solid state silicon detector (RAD7, Durrige Co. Inc., Bedford, MA, USA) or Radon Scout equipment (Sarad, Germany) were used to measure the indoor as well as the outdoor radon concentrations (Hassan et al., 2009; Catalano et al., 2015; Abdalla et al., 2019; Rafique et al., 2012; Matiullah et al., 2012). However, solid state nuclear track detectors (SSNTDs) such as CR-39, LR-115 or Makrofol can be inserted into a CAN-technique or Raduet (RadoSys Ltd., Budapest, Hungary), to measure indoor and outdoor

radon concentrations, as passive techniques (Hassan et al., 2009; Catalano et al., 2015; Abdalla et al., 2019; Rafique et al., 2012; Matiullah et al., 2012). The track detector method is extremely simple and does not require any high budget equipment unlike other technologies, while its accuracy is comparable to other methods, which gives it an advantage. In the present study, we use the CAN-technique equipped with solid state nuclear track detectors (SSNTDs) CR-39 to measure the in-situ and the laboratory radon concentrations after CR-39 detectors were precisely calibrated. Based on the measured in-situ radon concentration, the radiation dose was calculated and compared with the worldwide safety limit to confirm that Tanis city (archaeological site) has no radiation hazard. The radon emanation coefficient measured radon concentration in laboratory, and its exhalation rate were calculated and assessed.

EXPERIMENTAL DETAILS

Area of Study

San Al-Hagar (Tanis) is located at 150 km north-east of Cairo, (Figure. 1). Tanis is the Greek name of San Al-Hagar. Tanis is the most important archaeological site in northern Delta, Egypt. It is characterized by an eclectic reuse of materials that were usurped from other locations. It contains several temples such as; Ramses II, royal tombs and a sacred lake. About 2180 tourists from several countries all over the world (America, Belgium, Italy, Poland, Spain,.....etc.) Tanis every year.

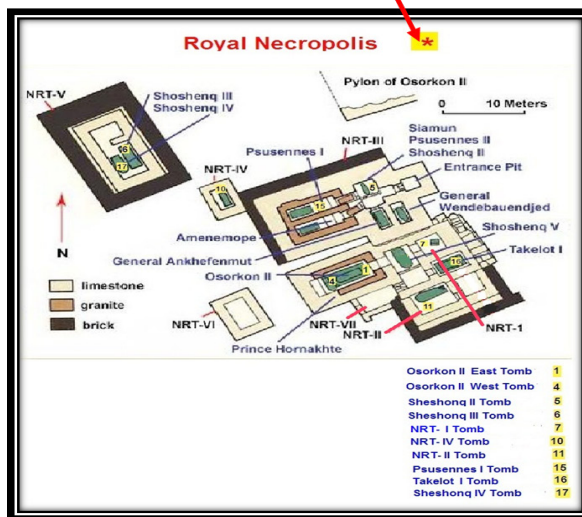
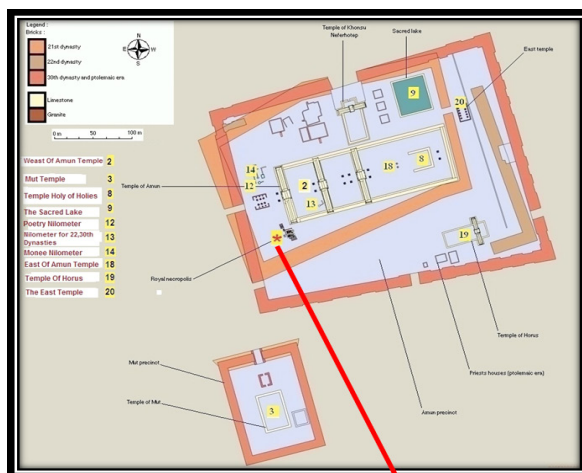


Fig. (1): The map of Tanis site.

Samples Preparation

Twenty samples of soil were collected from the surface layer within 5-10 cm of different locations at Tanis (San Al-Hagar), Sharqai, Egypt, i.e. the ground surface of tomb rooms, roads among tombs and from the empty outer space, as shown in Figure. (1). First, the samples were crushed and sieved through a 1 mm mesh size sieve to be more homogenous. Then, the samples were dried in an oven at a controlled temperature (110 °C) for a period of 24 hours to ensure complete dryness from moisture as any released radon is highly influenced by moisture content. After entire removal of moisture, the samples were placed into a desiccator and allowed to cool down to room temperature (Hassan et al., 2019). The ²²⁶Ra con-

centration in the selected samples for the present study was measured using an HPGe detector of vertical closed-end coaxial manufactured by Canberra. This detector has an accurately measured efficiency and an energy resolution of 2.1 keV at 1.33 MeV of γ -ray line of ^{60}Co (Egyptian Atomic Energy Agency, (EAEA), Cairo, Egypt). It was shielded with a cylindrical lead container of thickness 5 cm, which contains an inner concentric cylinder of Cu with a thickness of 10 mm, in order to reduce the effects of background. It was connected to a personal computer-based data acquisition system which has a Multi-Channel-Analyzer (8192 channels), to obtain γ -lines for interested radionuclides. For more information CAN be found elsewhere; (Hassan et al., 2019). The ^{226}Ra concentration for each sample is given in Table

1. The United Nations Scientific Committee on the Effects of Atomic Radiation (UNSCEAR, 1993) reported a typical ^{226}Ra concentration in soil should be in the range of 30 Bq kg^{-1} . All samples used in the present study have ^{226}Ra concentrations of less than 30 Bq kg^{-1} . Since radium concentration not only the factor that control the radon concentration in the atmosphere but also there other factors such as the texture and size of the grains, (e.g., macroscopic properties, crystallization of the grains' surfaces, and the texture and size of grains) and the permeability of the grains can influence on the level of radon in the atmosphere. Thus, its importance to measure the released radon concentration from the selected site in order to confirm that there is not radiation risk in that site.

Table (1) : Laboratory and In-situ radon concentration of archeological site (Tanis).

Location	Code of Sample	^{226}Ra Conc. (Bq kg^{-1})	Radon Conc. Lab. (Bq m^{-3})	Radon Conc. In site (Bq m^{-3})
Monee Nilometer	MN1	5.1 ± 3.3	115 ± 17	101 ± 12
Poetry Nilometer	PN1	7.8 ± 2.2	178 ± 28	144 ± 16
Nilometer for 22,30th Dynasties	ND1	7.2 ± 1.7	168 ± 19	141 ± 15
NRT I Tomb	NT1	4.4 ± 1.1	116 ± 16	81 ± 9
NRT II Tomb	NT2	4.9 ± 1.2	131 ± 16	91 ± 11
NRT IV Tomb	NT3	7.0 ± 3.1	157 ± 24	134 ± 14
Osorkon II East Tomb	OET1	4.1 ± 1.1	91 ± 10	78 ± 9
Osorkon II West Tomb	OWT1	4.7 ± 2.9	108 ± 14	87 ± 11
Sheshonq II Tomb	ST1	6.4 ± 1.3	141 ± 20	118 ± 12
Sheshonq III Tomb	ST2	6.5 ± 1.0	119 ± 18	121 ± 12
Sheshonq IV Tomb	ST3	3.9 ± 0.8	88 ± 12	72 ± 9
Psusennes I Tomb	PT1	5.3 ± 1.6	127 ± 14	109 ± 14
Takelot I Tomb	TT1	6.6 ± 2.1	151 ± 23	128 ± 14
The Sacred Lake	SL1	9.4 ± 1.6	226 ± 36	---
Temple Holy of Holies	THH1	8.4 ± 1.0	205 ± 33	---
Temple Of Horus	TH1	6.2 ± 1.9	137 ± 21	---
East Of Amun Temple	EAT1	5.5 ± 1.1	132 ± 16	---
West Of Amun Temple	WAT1	5.5 ± 0.2	133 ± 20	---
The East Temple	ET1	5.1 ± 1.7	117 ± 14	---
Mut Temple	MT1	5.3 ± 2.5	120 ± 14	---
Safety Limit		30	100 - 300	

Calibration process of CR-39 detectors equipped within the CAN-technique

To employ solid state nuclear track detectors (SSNTDs), CR-39 detector in CAN-technique to measure the radon concentration, the calibration coefficient of CR-39 detector should be measured firstly. The calibration coefficient of CR-39 is used to convert the alpha's track density (tracks cm^{-2}) to radon concentration in units of (Bq m^{-3}). Typically, the calibration coefficient of CR-39 detector [η], Tracks $\text{cm}^{-2}/(\text{Bq day m}^{-3})$] is defined as the relation between alpha's track density (produced from radon decay) to the integrated radon concentration in a closed volume. Calibration coefficient of the CR-39 detector depends on different factors such as the geometry of the using configuration, the registration sensitivity of the CR-39 detector, and radon concentration (Hassan et al., 2009). The calibration coefficient of the CR-39 detector CAN be measured by exposing the CR-39 detector to a known amount of integrated radon concentration inside a well-sealed chamber of a known volume.

During this work solid state nuclear track detectors (SSNTDs), Poly allyl diglycol carbonate (CR-39) detector was inserted in a CAN-chamber to measure radon concentration. CR-39 detector, of molecular composition $\text{C}_{12}\text{H}_{18}\text{O}_7$ and a density of 1.3 g/cm^3 , was supplied from Track Analysis System Ltd., UK (TASTRAK) Company. In our experiments, a sheet of CR-39 detector of thickness $700 \mu\text{m}$ was cut to pieces of area $1 \times 1 \text{ cm}^2$ for the measurements. Alpha Guard chamber, of 50-liters calibration chamber (supplied by Genitron, Germany), which is a non-leakage chamber in its sealed case (Hassan, 2014), was used as a well-sealed known volume chamber. During the calibration process, Alpha Guard radon monitor (standard monitor) was used to measure the radon concentration in the closed volume of the chamber as well as the temperature, humidity and pressure were also measured. In parallel, the CR-39 detector was fixed in an inverted cylindrical CAN-

chamber (3 cm diameter and 13 cm height, covered, at its bottom open mouth with a Whiteman fiber filter) was used to measure radon concentration (track density) of the same closed volume (Alpha Guard chamber). The Alpha Guard radon monitor and CR-39 detector as well as the radon source were all together equipped inside the Alpha Guard chamber, as seen in Fig.2.

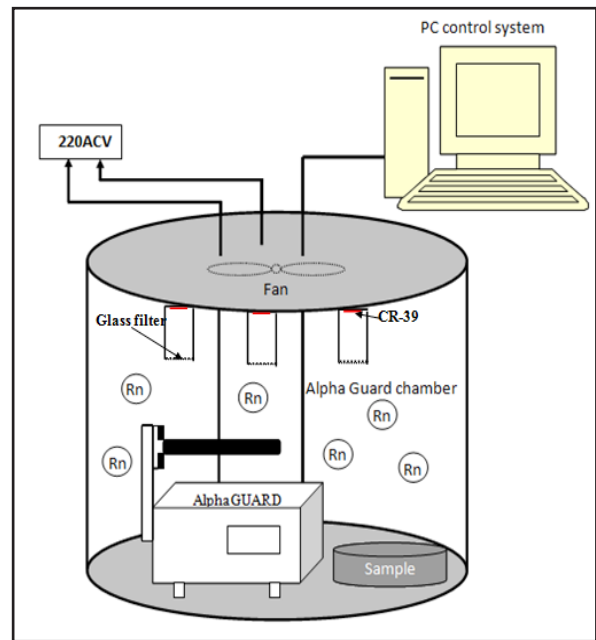


Fig. (2): Schematic diagram of the calibration process of CR-39 equipped in CAN-technique (Hassan, 2014).

The integrated radon concentration C_t ($C_t = \int_0^t C(t) dt$ Bq m^{-3} day) CAN be achieved by integrating the radon concentration $C(t)$ (measured with AlphaGuard radon monitor) over the exposure period (t) by using the following equation (Hafez et al., 2001).

$$C_t = C_0 \left(t - \frac{1 - \exp(-\lambda t)}{\lambda} \right) \quad (1)$$

Where, C_0 is the radon equilibrium concentration, which CAN be calculated from Eq. 2, t and λ are the exposure time and radon decay constant ($2.1 \times 10^{-6} \text{ s}^{-1}$).

$$C_0 = \frac{C(t)}{1 - \exp(-\lambda t)} \quad (2)$$

In-situ and laboratory radon concentration measurement

CR-39 detector was employed in the CAN-technique to measure in-situ and laboratory radon concentrations after its calibration coefficient was estimated. Typically, in the case of the in-situ measurement, a piece of CR-39 ($1 \times 1 \text{ cm}^2$) was fastened at the top of an inverted cylindrical CAN-chamber (3 cm diameter and 13 cm height) that covered at its bottom open mouth with a Whiteman fiber filter as shown in Fig.3a. After the CR-39 detectors is carefully equipped into CAN-chamber, both will be referred from now on as "CR-39-in-CAN-technique". The CR-39-in-CAN-technique was used to measure the released radon concentration at the under-investigation site (Fig. 3-a); a process called as the in-situ measurements.

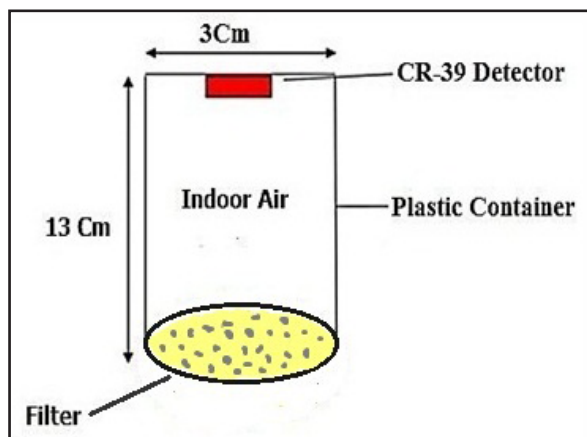


Fig. (3-a): Schematic Diagram for CAN-technique that will use in-situ measurements.

The CR-39-in-CAN-technique was attached to thirteen different locations at the archaeological site (Tanis, San Al-Hagar, Sharqai, Egypt), as seen in Fig.1. Typically, this CR-39-in-CAN-technique was fixed far away from both walls and ceiling by 1 m. After the thirteen CR-39-in-CAN-technique were set in the right position, they were left in their places for a period of 3 months (Fig. 1). Then (after that period), CR-39 detectors were carefully collected and etched in a NaOH solution of 6.25 M at a stable temperature of $70 \pm 0.5 \text{ }^\circ\text{C}$ (water bath) for 6 hours (Hassan et

al., 2013). Following the chemical etching process, all pieces were rinsed in running water for several minutes and washed with distilled water using the ultrasonic cleaner in order to totally terminate the etching process (removing all NaOH traces from the detector pores). The track density was counted using an optical microscope connected to a high-resolution digital camera with a fitting magnification of 400x.

In laboratory measurements a well prepared 20 soil samples were investigated to evaluate radon concentration using a sealed CAN-chamber equipped with CR-39 detector. The CAN-chamber is partitioned into two parts; one for a sample of the cylindrical container (of dimension of 3 cm in diameter by 7 cm in height), and the other for CR-39 (of dimension of 3 cm in diameter by 13 cm in height). A piece of CR-39 ($1 \times 1 \text{ cm}^2$) was fastened at the top of the inverted CAN-chamber, as seen in Fig. 3-b.

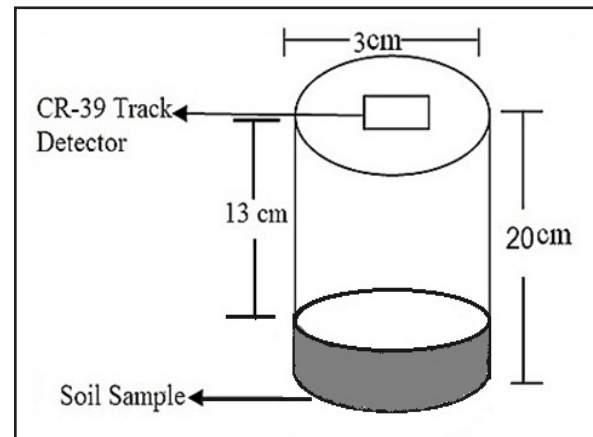


Fig. (3-b): Schematic Diagram for CAN-technique that will use in Laboratory measurements.

Then, each prepared sample was weighed and placed in a cylindrical container (bottom part) which was capped tightly to an inverted cylindrical 13 cm in height to avoid thoron gas concentration-effect because its diffusion length in atmospheric air is around 2.82 cm (EAPPEN et al., 2008). Thus, thoron activity is expected to decrease to about less than one-tenth after travelling a distance of 11.2 cm ($= 4 \times 2.82 \text{ cm}$). In this experimental system, the gap between the sample surface and detector was about 13 cm,

which suggests the thoron concentration around the detector decreases to less than 10%, compared with its value around the sample surface. The carefully sealed CANs were left for 3 months. During this time alpha particles from the decay process of radon hit the CR-39 detectors producing latent tracks. After the irradiation time, the exposed detectors were collected, etched and cleaned, and the track density was estimated (similar to the previously mentioned method).

RESULTS

The calibration process of CR-39 detectors equipped within the CAN-technique

The calibration coefficient of the CR-39 detector was precisely determined using three different radon sources of various concentrations (high, medium and low), which collected from three environmental materials of granite, scale waste, and phosphate with radium concentrations of 78571 ± 2362 , 10209 ± 510 and 1609 ± 164 Bq kg⁻¹, respectively, with a mass of 100-200 g each sample (Mansour et al., 2012; Hassan et al., 2013; Hassan et al., 2016). The two detectors of AlphaGuard monitor and CR-39 detector (placed at the top of an inverted CAN-chamber covered with a fiberglass filter on its open side) and a radon source (for instance, granite) were all together placed in AlphaGuard chamber, as shown in Fig. 2. Radon gas escaped from natural granite source $C(t)$ was recorded hourly using the AlphaGuard in its diffusion mode. Details of AlphaGuard monitor measurement in diffusion mode CAN be found elsewhere Hassan (Hassan, 2014). The previous procedure step was repeated again with another two-radon source of scale waste and phosphate. In parallel, the CR-39 records integrated alpha particle produced from the radon decay that released from granite radon source. The process of radon measurement within the AlphaGuard chamber using the aforementioned two detectors continues until the equilibrium concentration of radon is achieved ($C_0 = 11361$, 4352 and 2130 Bq m⁻³), as shown in Fig. 4.

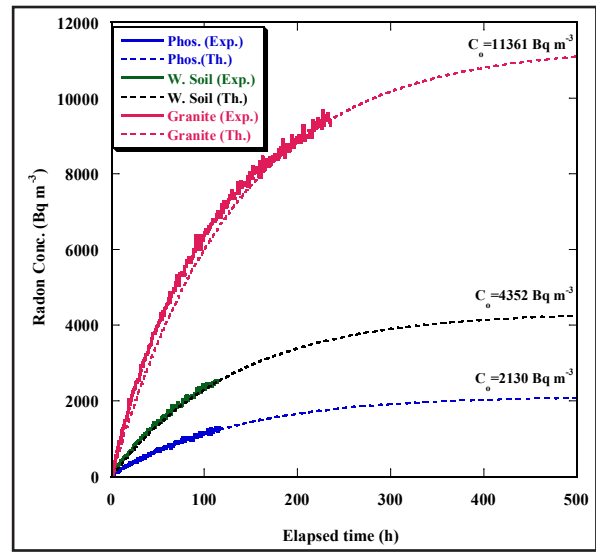


Fig. (4): Build up and equilibrium radon concentration in the sealed Alpha Guard chamber.

Accordingly, the integrated radon concentration in the sealed AlphaGuard chamber was simultaneously measured with an AlphaGuard monitor as well as with CR-39 detector (registered tracks of alpha particles of decayed radon atoms). The relation between the integrated radon concentration measured by AlphaGuard monitor and its corresponding track density measured with CR-39 detector is given in Fig. 5. From the calibration process of CR-39 detectors equipped within the CAN-technique; it was found that the registered alpha tracks increase as the integrated radon concentration increased, in a linear proportional equation of [track density (track cm⁻²) = 0.18 x (integrated radon conc. (Bq.m⁻³.day))] with a linear correlation coefficient of R= 0.99 (Fig. 5). Therefore, the calibration coefficient CAN be driven from the ratio between the registered tracks density (ρ_0) (track cm⁻²) and the integrated radon concentration according to Eq. 3.

$$\eta = \rho_0 / C_\tau \quad (3)$$

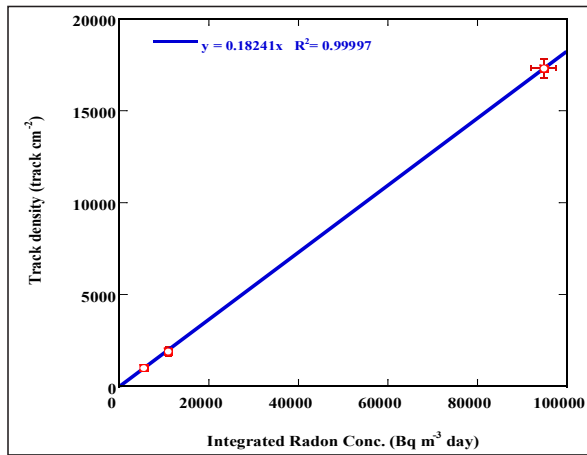


Fig. (5): The linear proportionality between the integrated radon concentration and the registered track in CR-39 detector.

Laboratory radon concentration measurement

In the laboratory, the equilibrium radon concentration was calculated from the alpha particle track density of radon that releases from each collected sample (Fig. 3-b) using Eq. 1 and 3. Equilibrium radon concentrations of 20 samples ranged from 88 ± 12 to 226 ± 36 Bq m⁻³ with a mean value of 139 ± 19 Bq m⁻³, Table 1. In addition to the radium content, it was found that a batch of factors are affect the variation in radon concentration. These factors are type of rock underlying the dwelling, double glazing, house type, floor level of rooms in which measurements were taken, window opening habits in the main bedroom, building materials used in the construction of the walls, floor type, and draught proofing. In addition, (Table 1) shows that the variation in radon concentration caused by another several factors; for instance the formation of a weathered soil sample from the temples, radium concentration in the samples, radium distribution in grains, the formation and the size of grains, and the variation of permeability among the samples (Somlai et al., 2008; Hassan et al., 2011). In addition, the internal structure of the materials (such as, macroscopic properties, crystallization of the grains' surfaces, and the texture and size of grains) also affects the released radon. For example, the radon level may be higher in case of crumbly grains rather than solid, even both particles have the same radium concentration (Hassan et al., 2011).

The radon surface exhalation rate of any sample, E , is defined as the flux of radon released from the surface of the material, was calculated from the following formula [10, 11].

$$E = \frac{C_q V \lambda}{S} \quad (4)$$

Where, λ is the decay constant of radon (2.1×10^{-6} s⁻¹), V is the volume of the air chamber, and S is the total surface area of the sample surface. We find the radon surface exhalation rate varies from $2.38 \pm 0.31 \times 10^{-5}$ (Bq m⁻² s⁻¹) to $6.12 \pm 0.97 \times 10^{-5}$ (Bq m⁻² s⁻¹) with a mean value of $3.76 \pm 0.52 \times 10^{-5}$ (Bq m⁻² s⁻¹), respectively, Table 2. Similar to the radon concentration, the variation in the radon surface exhalation rate from one sample to another is due to the same above-mentioned reasons (i.e. the properties of the sample, properties of grains and the radium distribution (Table 1) and its variation).

Comparison of radon concentration and radon exhalation rate for soil samples in present study with the reported values of famous tourist places in Egypt provide that it is higher than those reported places (Table 2).

Laboratory radon concentration measurement provided that, a strong correlation between the radon surface exhalation rate and radium content of the same sample with a linear correlation coefficient of ($y = 0.63x$, $R = 0.97$), Fig.6.

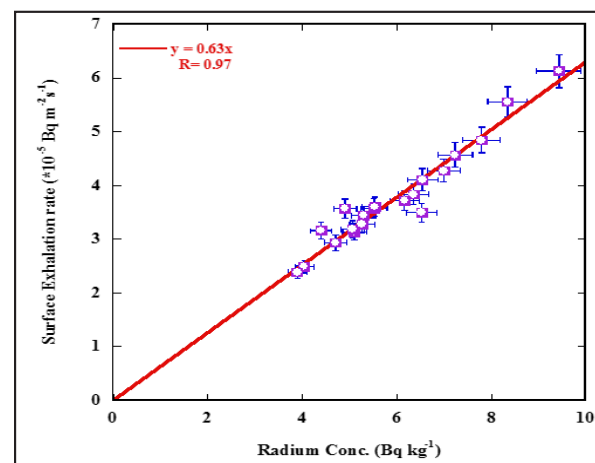


Fig. (6): The correlation between radon surface exhalation rate and radium content.

Table (2) : Comparison of radon concentration and radon exhalation rate for soil samples in present study with the reported values of famous tourist places in Egypt.

Countries	Radon Concentration (Bq m ⁻³)	Reference
(Alexandria)	72 ± 2.9	(El-Zaher, 2011 and 2013)
Tombs in the Saqqara region	(3,220 ± 227), (1,225 ± 286)	(Abo-Elmagd et al., 2006)
Tombs in the Saqqara region	(2,866 ± 37, 4,077 ± 72) & (1,286 ± 26, 2,394 ± 95) (1,571 ± 37, 3,882 ± 72)	(Salama et al., 2018)
Temsah Lake beach in Suez Canal region	29.40	(Fares, 2017)
Northern Safaga Bay	4.74	(El-Arabi et al., 2004)
Egypt (Tanis)	108 ± 12	Present study

Comparison of radon concentration and radon exhalation rate for soil samples in present study with the reported values of them in literature all over the

world showing that these two parameters are within the range of the reported values (Table 3).

Table (3) : Comparison of radon concentration and radon exhalation rate for soil samples in present study with the reported values of them in literature all over the world.

Countries	Radon Concentration (Bq m ⁻³)	Radon exhalation rate (Bq m ⁻² h ⁻¹)	Reference
Saudi Arabia (Jeddah)	36	6.42 ± 1.08	(Farid, 2016)
Pakistan (Islamabad)	64 ± 3.2	---	(Saeed et al., 2010)
Malaysia	98 ± 5.9	---	(Aswood, 2017)
Egypt (Alexandria)	72 ± 2.9	3.14	(El-Zaher, 2013)
Kosovo	128	---	(Gulan, 2017)
India (Punjab)	33.7 ± 1.4	0.04 ± 0.01	(Mehta, 2015)
Iraq (Baghdad)	45.5 ± 1.16	---	(Abdullah, 2013)
India (Hemavathi River)	374	---	(Kaliprasad et al., 2018)
Turkey (Sakarya)	9.2 ± 1.5	2.3 ± 0.6	(Adem, 2018)
Romania (Alba)	105 ± 5.2	---	(Muntean et al., 2014)
Kenya	170 ± 40	---	(Chege et al., 2009)
Egypt (Tanis)	108 ± 12	0.14 ± 0.02	Present study

The mass exhalation rate of radon of any sample, E_m , is defined as the flux of radon released from the unit mass of material, is calculated from the following formula [16].

$$E_m = (C_{eq} V \lambda) / M \quad (5)$$

Where, M is the total mass of the sample. We find the mass exhalation rate of radon of the measured samples gives the range value of $1.21 \pm 0.16 \times 10^{-7}$ (Bq kg⁻¹ s⁻¹) to $4.24 \pm 0.67 \times 10^{-7}$ (Bq kg⁻¹ s⁻¹) with a mean value of $2.37 \pm 0.33 \times 10^{-7}$ (Bq kg⁻¹ s⁻¹), respectively, as given in Table 4.

Table (4) : Radon surface and mass exhalation rate of the studied soil samples.

Soil Sample Code	Radon Surface Exhalation Rate $\times 10^{-5}$ (Bq m ⁻² s ⁻¹)	Radon Mass Exhalation Rate $\times 10^{-7}$ (Bq kg ⁻¹ s ⁻¹)
MN1	3.13 \pm 0.46	2.28 \pm 0.34
PN1	4.84 \pm 0.76	4.24 \pm 0.67
ND1	4.56 \pm 0.50	3.71 \pm 0.41
NT1	3.15 \pm 0.44	1.77 \pm 0.25
NT2	3.56 \pm 0.43	1.89 \pm 0.23
NT3	4.27 \pm 0.65	2.63 \pm 0.40
OET1	2.48 \pm 0.26	1.88 \pm 0.20
OWT1	2.93 \pm 0.39	2.34 \pm 0.31
ST1	3.83 \pm 0.53	1.98 \pm 0.28
ST2	3.49 \pm 0.49	1.64 \pm 0.23
ST3	2.38 \pm 0.31	1.21 \pm 0.16
PT1	3.44 \pm 0.38	2.20 \pm 0.24
TT1	4.10 \pm 0.63	2.40 \pm 0.37
SL1	6.12 \pm 0.97	4.06 \pm 0.64
THH1	5.55 \pm 0.90	2.83 \pm 0.46
TH1	3.71 \pm 0.57	2.35 \pm 0.36
EAT1	3.57 \pm 0.43	2.00 \pm 0.24
WAT1	3.60 \pm 0.53	2.15 \pm 0.32
ET1	3.18 \pm 0.38	1.96 \pm 0.23
MT1	3.27 \pm 0.38	1.78 \pm 0.21

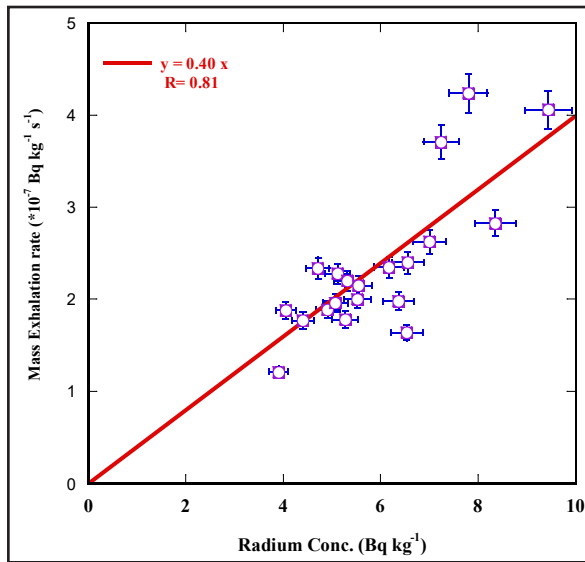


Fig. (7): The correlation between radon mass exhalation rate and radium content.

This correlation confirms that the radon gas in the atmosphere depends on the radium content of those samples. Thus, radium content is a useful index of radon exhalation rate (both surface and mass).

In-situ radon concentration measurement

In-situ measurements of radon concentration, in 13 sites at Tanis, San Al-Hagar (archaeological city), Sharqia, Egypt, was carried out using CAN-technique. For these in-situ measurements, the CAN-chamber was equipped at its top part with CR-39 (Fig. 3-a) that has a covered bottom open mouth with a glass filter. The radon gas released collectively from all content materials at the under study location was diffused within this closed air volume in the CAN-chamber (Fig. 3-a). Once the radon release from the environment materials in the site, it enters in the CAN-chamber and starts to decay, the alpha particle produced from the radon decay process will create an alpha track in the CR-39 detector. This alpha track CAN be manually counted under an optical microscope. In-situ radon concentration is equal to the multiplication of track density by the calibration factor of CR-39 (see Eqs. 1 & 3). The value of the in-situ radon concentration varied of 72 ± 9 to 144 ± 16 Bq m⁻³ with a mean value of 108 ± 12 Bq m⁻³ (Table

1). This variation of radon concentration in different sites is due to the variance of their composition of limestone, bricks and granite rocks. Consequently, the radium content will be varied from a material to another (Table 1). We find the radon concentrations in the studied archaeological site are less than the safety limit of 100-300 Bq m⁻³ reported by (ICRP, 2010; WHO, 2005).

Based on the measured values of the in-situ radon concentration from different locations at Tanis site and the exposure time by the site's guides and visitors to radon, the annual effective dose due to exposure to radon was calculated using Eq. (6), (Papachristodoulou et al., 2004; Özen et al., 2018).

$$E = C_{Rn} \cdot F \cdot t \cdot d \cdot u \quad (6)$$

where, E, effective dose (mSv y⁻¹), C_{Rn}, the in-situ radon concentration (Bq m⁻³), F, equilibrium factor between radon and its decay products (F= 0.4), t, the annually spent time in the location (h y⁻¹), d, dose conversion factor (1.4 mSv per mJ h m⁻³), u, unit conversion factor [$5.6 \cdot 10^{-6}$ mJ m⁻³ per Bq m⁻³ (ICRP, 1993 and 2017)]. The radiation dose calculations were carried out with the assumption that visitors remain for about one hour inside the location during each guided tour. In contrast, the guides spend the working hours inside the location as ($0.2 \cdot 8760$ h y⁻¹ = 1752 h y⁻¹). The annual effective radiation dose was varied from 0.40 ± 0.05 to 0.79 ± 0.09 mSv y⁻¹ with a mean value of 0.59 ± 0.07 mSv y⁻¹ for the guides, while its value was ranged from 0.054 ± 0.007 to 0.108 ± 0.012 mSv y⁻¹ with a mean value of 0.081 ± 0.009 mSv y⁻¹ for the visitors (tourists), respectively, as seen in Table 2. The obtained results imply that the received radiation dose to both guides and visitor is much lower than the recommended value annual effective radiation dose due radon of 3-10 mSv y⁻¹, (ICRP, 2010), and is also less than the recommended value by (UNSCEAR, 2008), of the worldwide average dose due to inhalation of radon 1.15 mSv y⁻¹.

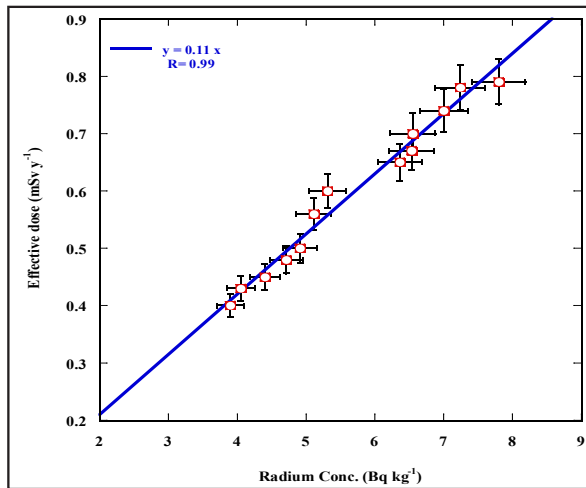


Fig. (8): The correlation between effective radiation dose and radium content.

Table (5) : Effective dose of releasing radon from the soil.

Soil Sample Code	Effective dose For Guides (mSv y ⁻¹)	Effective dose For Visitors (mSv y ⁻¹)
MN1	0.56 ± 0.06	0.076 ± 0.009
PN1	0.79 ± 0.09	0.108 ± 0.012
ND1	0.78 ± 0.08	0.106 ± 0.011
NT1	0.45 ± 0.05	0.061 ± 0.006
NT2	0.50 ± 0.06	0.068 ± 0.008
NT3	0.74 ± 0.07	0.101 ± 0.010
OET1	0.43 ± 0.05	0.058 ± 0.007
OWT1	0.48 ± 0.06	0.066 ± 0.008
ST1	0.65 ± 0.07	0.089 ± 0.009
ST2	0.67 ± 0.07	0.091 ± 0.009
ST3	0.40 ± 0.05	0.054 ± 0.007
PT1	0.60 ± 0.07	0.082 ± 0.010
TT1	0.70 ± 0.08	0.096 ± 0.010
Safety Limit		3 - 10 mSv y ⁻¹ (ICRP, 2010)

DISCUSSION

The calibration coefficient of the CR-39 detector was found to be 0.18 ± 0.01 Alpha tracks cm⁻² per (Bq.m⁻³.day) which enable this system to be applicable in national surveys of radon concentrations.

The results of the current study is agree with the reported values, in the literature, for the calibra-

tion coefficient of the CR-39 detector equipped with the similar geometry. For example, (Abo-Elmagd, 1997; Hafez et al., 2001; Hassan et al., 2009) reported the calibration coefficient of CR-39 values of 0.18 ± 0.02 , 0.18 ± 0.01 , and 0.17 ± 0.03 Alpha tracks cm⁻² per (day Bq m⁻³), respectively.

Table 5 introduce effective dose of releasing radon from the soil depending on the coded samples and hence calculating the yearly effective dose for both of guides and visitors; showing that it is much lower than the safety limits of ICRP.

Fig. (6) show the strong correlation between radon surface exhalation rate and radium content, that may reflect the dependence of radon gas in the atmosphere on the radium content of these samples so that radium content could be a good index to predict the radon surface exhalation rate. Moreover, the mean measured values of the radon surface exhalation rate in the present study were shown in agreement with the reported values in the literature from various sites around the world, as shown in Table 3.

The radon mass exhalation is also controlled by the properties of the sample, properties of grains and the radium distribution (Table 1) and its variety. A good correlation was also noticed between the radon mass exhalation rate and radium content of the same samples with a linear correlation coefficient of ($y = 0.4 x$, $R = 0.81$), as shown in Fig.7.

In-situ radon concentration measurement introduced a strong linear correlation between the annual effective dose and a sample's radium content, collected from the same understudy locations, with a correlation coefficient of ($y = 0.11 x$, $R = 99$), Fig.8.

This strong correlation suggests the dependence of radiation dose on the radium content, and therefore, one CAN conclude that the soil is the primary source of radon in the atmosphere (Table 5).

Depend on all above; we can conclude that the radium concentration in the collected samples is a useful index for both all radon parameters and the annual effective dose. Therefore, the radium concentration value can be used as a screening indicator for the radiation dose at any archaeological site (Hassan et al., 2020). Based on the results and findings of this study, the authors confirm that there is no radiation risk to both the guides and the tourists at (Tanis, San Al-Hagar, Sharqai, Egypt) site. The authors encourage tourists from all over the world

to visit the Tanis archaeological site, Egypt.

CONCLUSIONS

The in-situ and laboratory radon concentrations at Tanis, Egypt were measured using CAN-technique equipped with a precisely calibrated CR-39 of the calibration coefficient of 0.18 ± 0.01 alpha track. cm^2 per $\text{Bq.m}^{-3}.\text{day}$. The in-situ radon concentration ranged from 72 ± 9 to 144 ± 16 Bq m^{-3} with a mean value of 139 ± 19 Bq m^{-3} . In comparison, the laboratory radon concentration varied from 88 ± 12 to 226 ± 36 Bq m^{-3} with a mean value of 108 ± 12 Bq m^{-3} . A strong correlation is noticeable between the in-situ and the laboratory radon concentration with a linear correlation factor of $R = 0.92$ and a linear equation of (in-situ radon concentration = $0.8 \times$ laboratory radon concentration), which implies a good accuracy of this study's proposed technique. Moreover, the average value of radon concentration at Tanis is less than the recommended value of 100 and 300 Bq m^{-3} . Furthermore, the radon exhalation rate was ranged from 23.8 ± 3.1 to 61.2 ± 9.7 $10^{-4}(\text{Bq m}^{-2} \text{ s}^{-1})$. A radon exhalation rate was also strongly correlated to radium content with a linear correlation factor of $R = 0.97$ in an equation of (radon exhalation rate = $0.6 \times$ radium content). In addition, we find the annual effective dose of radon exposure from Tanis site extend from 0.40 ± 0.05 to 0.79 ± 0.09 mSv y^{-1} for guides and from 0.054 ± 0.007 to 0.108 ± 0.012 mSv y^{-1} for visitors. The radiation dose is strongly correlated to the radium content of the collected samples, which implies that the releasing radon from soils is the main contributor of the delivered radiation dose. Our results imply that there is no radiation health hazard at Tanis archaeological site. This means that; the site is safe for tour guide and visitors.

ACKNOWLEDGMENTS

The authors expressed their appreciation and thanks to prof. Dr. N. A. Mansour, physics department, faculty of science, Zagazig University, Egypt

for his comments and supporting us with his laboratory tools in order to carry out this work.

REFERENCES

- **Abdalla, A.M. and Al-Naggar, T.I. (2019):** Estimation of radiologic hazards of radon resulting from ceramic tiles used in Najran city. *J. Radiat. Res. Appl. Sci.*, 12: 210-218.
- **Abdullah, A.M. (2013):** Concentration Measurements of Radon, Uranium and Background of Gamma Rays in Air at the University of Baghdad, Al-Jadiriya Site. *Journal of Baghdad for Science, Iraq.*
- **Abo-Elmagd, M. (1997):** Calibration and concentration measurement of radon gas in radon gas chamber. M.Sc. Thesis, Physics department, Faculty of science, Ain Shams University, Cairo, Egypt.
- **Abo-Elmagd, M.; Metwally, S.M.; Elmongy, S.A.; Salama, E. and El-Fiki, S.A. (2006):** External and internal exposure to natural radiations inside ancient Egyptian tombs in Saqqara, *Radiation Measurements* 41, 197–200.
- **Abo-Elmagd M.; Saleh, A. and Afifi, G. (2018):** Evaluation of radon related parameters in environmental samples from Jazan city, Saudi Arabia, *J. Radiat. Res. Appl. Sci.*, 11: 104-110.
- **Adem, K. (2018):** Measurement of the radon exhalation rate and effective radium concentration in soil samples of southern Sakarya, Turkey. *Indoor and Built Environ.*, 27: 278-288.
- **Aswood, M.S. (2017):** Estimation of Radon Concentration in Soil Samples from Cameron Highlands, Malaysia, *East Asian Science Technology and Society an International Journal*, 5, 9:12.
- **Catalano, R.; Imme, G.; Mangano, G.; Morelli, D.; Aranzulla, M.; Giammanco, S. and Thinova, L. (2015):** In situ and laboratory measurements for radon transport process study, *J. Radioanal. Nucl. Chem.*, 306: 673-684.
- **Chege, M.W.; Rathore, V.S.; Chhabra, S.C. and Mustapha, A.O. (2009):** The influence of meteorological parameters on indoor radon in selected traditional Kenyan dwellings, *J. Radiol. Prot.*, 29: 95-103.
- **Durrani, S.A. and Bull, R.K. (1987):** Solid State Nuclear Track Detection: Principles, Methods and applications, Pergamum Press, Oxford.
- **Eappen, K.P.; Sahoo, B.K.; Ramachandran, T.V. and Mayya, Y.S. (2008):** Calibration factor for thoron estimation in cup dosimeter, *Radiat. Meas.*, 43: S418-S421.
- **El-Arabi, A.M.; El-Saman, M.I.; Maiyya, I.A.; Tartor, B.A. and Bashter, I.I. (2004):** Radon Concentration and its Relation with some Environmental Conditions in the Northern Safaga Bay, VII Radiation Physics & Protection Conference, 27-30 November 2004, Ismailia-Egypt.
- **El-Zaher, M. (2011):** Seasonal variation of indoor radon concentration in dwellings of Alexandria city, Egypt, *Radiation Protection Dosimetry*, 143(1): 56:62.
- **El-Zaher, M. (2013):** A comparative study of the indoor radon level with the radon exhalation rate from soil in Alexandria city. *Radiat. Prot. Dosim.*, 154: 490-496.
- **Fares, S. (2017):** Measurements of natural radioactivity level in black sand and sediment samples of the Tamsah Lake beach in Suez Canal region in Egypt, *Journal of Radiation Research and Applied Sciences* 10.
- **Farid, S.M. (2016):** Indoor radon in dwellings of Jeddah city, Saudi Arabia and its correlations with the radium and radon exhalation rates from soil. *Indoor and Built Environ.*, 25: 269=278.
- **Gulan, L. (2017):** Is high indoor radon concentration correlated with specific activity of radium in nearby soil? A study in Kosovo and Metohija, *Environ. Sci. Pollut. Res.*, 24: 19561.

- **Hafez, A.F.; Hussein, A.S. and Rasheed, N.M. (2001):** A study of radon and thoron release from Egyptian building materials using polymeric nuclear track detectors. *Appl. Radiat. Isot.*, 54: 291.
- **Hassan, N.M. and Kim, Y.J. (2020):** A feasibility test for quick radon risk assessment by measuring an in-situ radiation dose. *Radiat. Prot. Dosim.*, 192 (4): 482.
- **Hassan, N.M. and Hafez, A.F. (2013):** Studying the Physical Parameters of a Solid-State Nuclear Track Detector, *J. Korean. Phys. Society.*, 63: 1713.
- **Hassan, N.M. (2014):** Radon emanation coefficient and its exhalation rate of wasted petroleum samples associated with the petroleum industry in Egypt. *J. Radioanal. Nucl. Chem.*, 299: 111.
- **Hassan, N.M.; Hosoda, M.; Ishikawa, T.; Sorimachi, A.; Sahoo, S.K.; Tokonami, S. and Fukushi, M. (2009a):** ²²²Rn Exhalation Rate from Egyptian Building Materials Using Active and Passive Methods. *Jpn. J. Health Phys.*, 44: 106.
- **Hassan, N.M.; Hosoda, M.; Ishikawa, T.; Sorimachi, A.; Sahoo, S.K.; Tokonami, S. and Fukushi, M. (2009b):** Radon Migration Process and Its Influence Factors; Review. *Jpn. J. Health Phys.*, 44: 218.
- **Hassan, N.M.; Ishikawa, T.; Hosoda, M.; Iwaoka, K.; Sorimachi, A.; Sahoo, S.K.; Janik, M.; Kranrod, C.; Yonehara, H.; Fukushi, M. and Tokonami, S. (2011):** The effect of water content on the radon emanation coefficient for some building materials used in Japan. *Radiat. Meas.*, 46: 232.
- **Hassan, N.M.; Mansour, N.A. and Fayez-Hassan, M. (2013):** Evaluation of radionuclide concentrations and associated radiological hazard indexes in building material used in Egypt. *Radiat. Prot. Dosim.*, 157: 214.
- **Hassan, N.M.; Mansour, N.A.; Fayez-Hassan, M. and Sedqy, E. (2016):** Assessment of natural radioactivity in fertilizers and phosphate ores in Egypt. *J. Taibah University for Science*, 10: 296.
- **Hassan, N.M.; Mansour, N.A.; Salama, S. and Al-deeb A. (2019):** Estimation of Radiation Hazards of Natural Radionuclides in Archaeological Site (Tanis), Egypt. *Arab J. Nucl. Sci Appl.*, 52: 62.
- **Hosoda, M.; Sorimachi, A.; Yasuoka, Y.; Ishikawa, T.; Sahoo, S.K.; Furukawa, M.; Hassan, N.M.; Tokonami, S. and Uchida, S. (2009):** Simultaneous measurement of radon and thoron exhalation rates and comparison with values calculated by UNSCEAR equation. *J. Radiat. Res.*, 50: 333.
- **ICRP, (2010):** International Commission of Radiological Protection ICRP. Lung Cancer risk from radon and progeny and statement on radon. ICRP Publication 115 *Annals of the ICRP*, 40(1): 1.
- **ICRP, (1993):** (International Commission on Radiological Protection), Protection against radon-222 at home and at work. Oxford: Pergamon Press; Publication 65.
- **ICRP, (2017):** (International Commission on Radiological Protection), Occupational intakes of radionuclides: Part 3. (ICRP Publication 137; *Ann. ICRP* 46 (3/4).
- **Kaliprasad, C.S. and Yerol, N. (2018):** Radon concentration in water, soil and sediment of Hemavathi River environments. *Indoor and Built Environ.*, 27(5): 587.
- **Mansour, N.A.; Ahmed, T.S.; Hassan, M.F.; Hassan, N.M.; Gomaa, M.A. and Ali, A. (2012):** Measurements of radiation level around the location of NORM in solid wastes at petroleum companies in Egypt. *J. American Science*, 8(6): 252.
- **Matiullah, M.; Malik, F. and Rafique, M. (2012):** Indoor radon monitoring near an in-situ leach mining site in D G Khan, Pakistan. *J. Radiol. Prot.*, 32(4): 427.
- **Mehta, V. (2015):** Study of Indoor Radon, Thoron, Their Progeny Concentration and Radon Exhalation Rate in the Environs of Mohali, Punjab, Northern India. *Aerosol Air Qual. Res.*, 15: 1380.

- **Muntean, L.E.; Cosma, C.; Cucos, A.; Dicu, T. and Moldovan, D.V. (2014):** Assessment of annual and seasonal variation of indoor radon levels in dwelling house from Alba country, Romania, ROMANIA, Rom. J. Phys., 59: 163.
- **Nazaroff, W.W. (1992):** Radon transport from soil to air. Rev. Geophys., 30: 137.
- **Özen, S.A.; Çevik, U. and Taşkın, H. (2018):** Comparison of active and passive radon survey in cave atmosphere, and estimation of the radon exposed dose equivalents and gamma absorbed dose rates, Isot. Environ. Health Studies, 55: 92.
- **Papachristodoulou, C.A.; Ioannides, K.G.; Stamoulis, K.C.; Patiris, D.L. and Pavlides, S.B. (2004):** Radon activity levels and effective doses in the Perama cave, Greece, Health Phys., 86: 619.
- **Rafique, M.; Rahman, S.U. and Akram, M. (2012):** Estimation of concentration and exposure doses due to radon by using CR-39 plastic track detectors in the residences of Sudhnuti, Azad Kashmir, Pakistan. Environ. Earth Sci., 66(4): 1225.
- **Saeed, U.R.; Rafique, M.; Matiullah; and Anwar, J. (2010):** Radon measurement studies in workplace buildings of the Rawalpindi region and Islamabad Capital area, Pakistan. J. Building and Environ., 45: 421.
- **Sahu, P.; Panigrahi, D.C. and Mishra, D.P. (2016):** A comprehensive review on sources of radon and factors affecting radon concentration in underground uranium mines. Environ. Earth. Sci., 75: 617.
- **Salama, E.; Ehab, M. and Rühm, W. (2018):** Radon and thoron concentrations inside ancient Egyptian tombs at Saqqara region: Time-resolved and seasonal variation measurements. Nucl. Eng. Technol., 50(6): 950.
- **Sasaki, T.; Gunji, Y. and Okuda, T. (2004):** Mathematical modeling of radon emanation. J. Nucl. Sci. Technol., 41: 142.
- **Schery, S.D.; Wilkening, M.H.; Hart, K.P. and Hill, S.D. (1989):** The flux of radon and thoron from Australian soils. J. Geophys. Res., 94: 8567.
- **Somlai, J.; Somlai, K.; Jobbágy, V.; Kovács, J.; Németh, C. and Kovács, T. (2008):** Connection between radon emanation and some structural properties of coal slag as building material. Radiat. Meas., 43: 72.
- **UNSCEAR, (2000):** Sources and effects of ionizing radiation. Report to the General Assembly, with Scientific Annexes (New York: UNSCEAR).
- **UNSCEAR, (1993):** Sources and effects of ionizing radiation. Report to the General Assembly, with Scientific Annexes (New York: UNSCEAR).
- **UNSCEAR, (2008):** Sources and effects of ionizing radiation. Report to the General Assembly, with Scientific Annexes, United Nations.
- **WHO, (2005):** Fact Sheet No. 291: Radon and Cancer.